Strain Posavljak

PRORAČUN OŠTEĆENJA DISKOVA AVIONSKIH MOTORA
DAMAGES COMPUTATION OF AIRCRAFT ENGINE DISKS

Originalni naučni rad / Original scientific paper
UDK /UDC: 629.7.036, 621.45
Rad primljen / Paper received: 22.04.2009.

Adresa autora / Author's address:
„ORAO“ a.d. Sabackih djaka bb, 76300 Bijeljina, Republic of Srpska, Bosnia and Herzegovina, oraoi@rstel.net

Ključne reči
- diskovi avionskih motora
- motorski start-stop ciklus
- naponsko-deformacijski odziv
- približna Sonsinoova kriva
- proračun oštećenja

Izvod

Problem oštećenja diskova avionskih motora, pretežno opterećenih centrifugalnim silama lopatica i sopstvenim centrifugalnim silama, razmatran je u ovom radu. Disk prvog stepena rotora kompresora niskog pritiska motora R25-300 izabran je kao predstavnik ovih diskova. Primenom Palmgrin-Majnerove hipoteze o linearnoj akumulaciji oštećenja izveden je proračun oštećenja ovog diska za jedan start-stop ciklus motora. Pri tome je radni spektar amplituda deformacija u tački očekivanog iniciranja prsline, identifikovan pomoću približnih Sonsinoovih krivih, doveden u vezu sa Morouvim krivim niskocikličnog zamora.

UVOD

Diskove avionskih motora u toku rada opterećuju centrifugalne sile lopatica, sopstvene centrifugalne sile, direktne gasodinamičke sile i gasodinamičke sile koje deluju na lopatice, a momenti inercije lopatica, sopstveni momenti inercije i temperatura su uticajni faktori. Centrifugalne sile su dominantne kod diskova ventilatora, diskova kompresora niskog pritiska i diskova nižih stepena kompresora visokog pritiska. Kod diskova viših stepena kompresora visokog pritiska i turbinskih diskova, sem centrifugalnih sila, treba uzeti u obzir i termička opterećenja, dok se ostala opterećenja mogu zanemariti. Centrifugalne sile su stohastički promenljive u zavisnosti od izvedenih letova i provera motora na zemlji. Letovi i provere motora na zemlji se mogu opisati start-stop ciklusima definisanim i praćenim na više načina. Za diskove pretežno opterećene centrifugalnim silama lopatica i sopstvenim centrifugalnim silama značajni su start-stop ciklusi, definisani blokovima učestanosti obrtanja. Takvi start-stop ciklusi izazivaju oštećenja, zbog kojih se na kritičnim mestima diskova iniciraju zamorne prsline, /1-5/. Prsline ove vrste rezultat su niskocikličnog zamora, čije su glavno obeležje elasto-plastične deformacije.

Proračun oštećenja konkretnog diska podrazumeva poznavanje start-stop ciklusa motora, prostih ciklusa unutar njih, cikličnih karakteristika ugrađenog ili izabranog materijala i naponsko-deformacijski odziv u tački očekivanog iniciranja prsline za sve proste cikluse.

Keywords
- aircraft engine disks
- engine start-stop cycle
- stress-strain response
- approximate Sonsino’s curve
- damages computation

Abstract

The problem of damages of aircraft engine disks, dominantly loaded by centrifugal forces of blades and own centrifugal forces is considered in this paper. The first stage low pressure compressor rotor disk of R25-300 engine has been chosen as the representative of these disks. Using Palmgreen-Miner’s hypothesis on linear accumulation of damages, damage computation of this disk for one engine start-stop cycle, was performed. During that, the spectrum of working strain amplitudes, at the point of expected crack initiation, identified by approximate Sonsino’s curves, is related with Morrow’s curves of low cycle fatigue.

INTRODUCTION

Aircraft engine disks are in operation loaded by centrifugal forces of blades, centrifugal forces of disks alone, direct gas dynamic forces and gas dynamic forces acting on blades, and the influencing factors are moments of inertia of blades, moments of inertia of the disks and temperature. Centrifugal forces are dominant for disks of fans, disks of low pressure compressors and disks of lower stages of high-pressure compressors. For disks of higher stages of high pressure compressors and for turbine disks, except centrifugal forces, thermal loads must be taken in account, while remaining loads can be neglected. Centrifugal forces are stochastically variable, depending on realized flights and engine ground inspections. Flights and engine ground inspections can be described by start-stop cycles defined and observed in different ways. For disks dominantly loaded by centrifugal forces of blades and own centrifugal forces, start-stop cycles defined by blocks of rotation frequency are important. Such start-stop cycles produce damages, responsible for fatigue cracks initiation in critical regions, /1-5/. Cracks of this kind are the result of low cycle fatigue with elasto-plastic strains as the main feature.

Damage computation of the actual disk includes the information of engine start-stop cycles, simple cycles inside them, cyclic properties of used or specified material and stress-strain response in the point of expected crack initiation for all simple cycles.

Naponsko-deformacijski odziv u tački očekivanog iniciranja prsline za sve proste cikluse i metoda njihovog prebrojavanja unutar start-stop ciklusa motora posebno su važni. Od tačnosti jednog i drugog zavisi tačnost proračuna oštećenja. Za identifikaciju prostih ciklusa unutar start-stop ciklusa motora mogu se primeniti metoda ciklusa kišnog toka, metoda parnih raspona, /6, 7/, i metoda rezervoara, /8/. Korišćenjem metoda konačnih elemenata, elektrootpornih mernih traka ili pak Nojberovog pravila u standardnom ili modifikovanom obliku, /6, 7/, mogu se odrediti naponsko-deformacijski odzivi.

Postupak proračuna oštećenja diska prvog stepena rotora kompresora niskog pritiska avionskog motora R25-300 za jedan motorski start-stop ciklus izložen je u ovom radu.

DISK PRVOG STEPENA ROTORA KOMPRESORA NISKOG PRITISKA AVIONSKOG MOTORA R25-300

Osnovni podaci o disku

Radni vek diska prvog stepena rotora kompresora niskog pritiska avionskog motora R25-300, ovde označenog sa D1, je propisan na nivou 1200 časova leta, /9/. Disk je u sklopu sa drugim elementima rotora prikazan na sl. 1. Propisani radni vek nije dostignut zbog prevremenih prslina. Prevremena prslina na jednom disku D1 data je na sl. 2, /10/.

Stress-strain response at the point of expected crack initiation for all simple cycles and method of their counting inside of engine start-stop cycles are of special importance. The accuracy of the overall damage computation will depend on the accuracy of both. For identification of simple cycles inside of engine start-stop cycles, the method of rain flow cycle count, the range pair method /6, 7/ and alike, good method of reservoir /8/ are applicable. Using the finite element method, strain gauges or Neuber's rule in standard or modified form, /6, 7/, the stress-strain responses can be identified.

The procedure of damage computation of the first stage low pressure compressor rotor disk of R25-300 aircraft engine for one engine start-stop cycle is shown in the paper.

THE FIRST STAGE LOW PRESSURE COMPRESSOR ROTOR DISK OF R25-300 AICRAFT ENGINE

The basic data about disk

The service life of the first stage low pressure compressor rotor disk of R25-300 aircraft engine, here designed as D1, is specified for 1200 flight hours /9/. The disk, assembled with the other rotor elements, is presented in Fig. 1. Specified service life is not achieved due to premature cracks. Premature crack on one D1 disk is shown in Fig. 2, /10/.

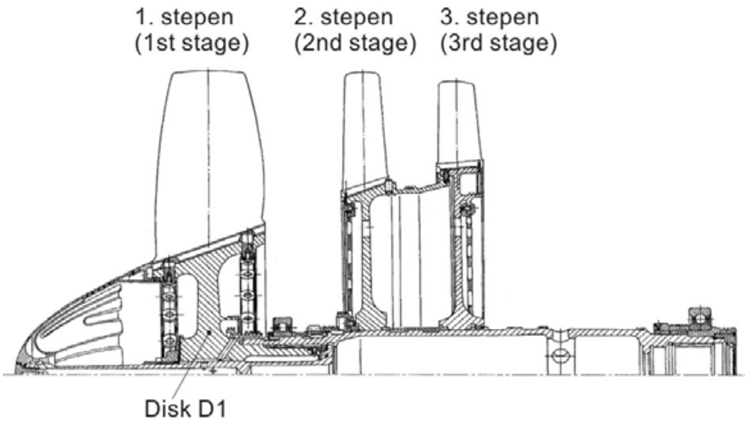

Slika 1. Disk D1 u sklopu sa ostalim elementima rotora
Figure 1. Disk D1 in assembly with other rotor elements.

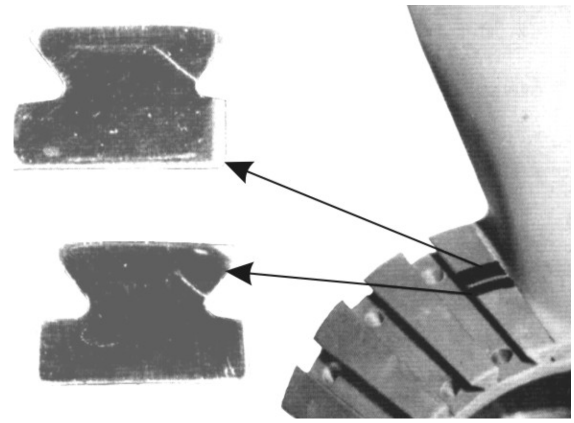

Slika 2. Primer prevremene prsline na jednom disku D1
Figure 2. Example of premature crack on one disk D1.

Posle reklamacija, proizvođač motora R25-300 je na osnovu biltena /11/ u eksploataciju uveo novi rekonstruisani disk D2 prvog stepena rotora kompresora niskog pritiska.

Rekonstrukcija se prema sl. 3 sastoji u povećanju debljine zadnjeg dela oboda i promeni oblika čivija za fiksiranje lopatica. Očekivalo se da će propisani radni vek od 1200 časova leta biti dostignut sa diskom D2. Međutim, to se nije dogodilo. Prevremene prsline su se, na istom mestu kao i na disku D1, pojavljivale i na disku D2. Statističkom obradom podataka o ultrazvučno otkrivenim prslinama dobijeni su Vejbulovi izrazi za verovatnoće iniciranja prslina $P_1(t)$ na disku D1 i $P_2(t)$ na disku D2.

After complaints, the producer of R25-300 engine, based on Bulletin /11/ has introduced in service new re-designed disk D2 of the first stage low pressure compressor rotor.

Redesign according to Fig. 3 consisted in strengthening of rim back part and in change of shape of pins for blade fixing. It was expected that the specified service life of 1200 flight hours would be reached with disk D2. However, this did not happen. Premature cracks, at the same location as on disk D1, have initiated on disk D2. By statistical data processing about cracks detected by ultrasonics, Weibull's expressions for probabilities of cracks initiation $P_1(t)$ on disk D1 and $P_2(t)$ on disk D2 were obtained.

$$P_1(t)=1-e^{-\left(\frac{t}{356}\right)^{3.4172}} \text{ on disk D1, and } \quad P_2(t)=1-e^{-\left(\frac{t}{356}\right)^{2.764}} \text{ on disk D2} \tag{1}$$

Iz grafičkog prikaza jed. (1) na sl. 4. vidi se da je disk D2 lošiji od svog prethodnika, diska D1.

From the graphical presentation of Eq. (1) in Fig. 4 it is clear that disk D2 is worst then its predecessor, disk D1.

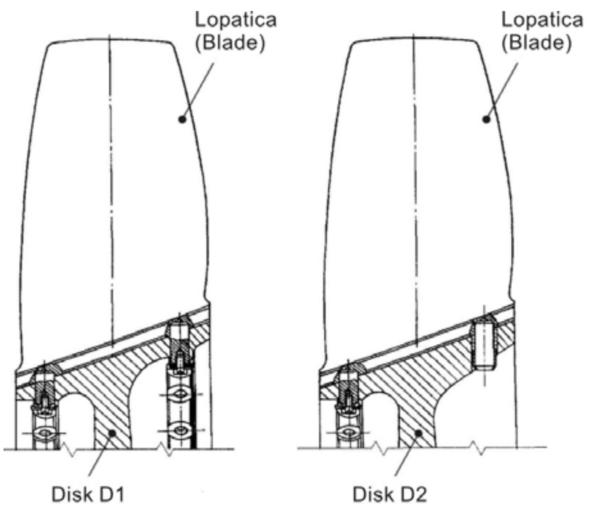

Slika 3. Ilustracija razlike diskova D1 i D2
Figure 3. Illustration of differences in disks D1 an D2.

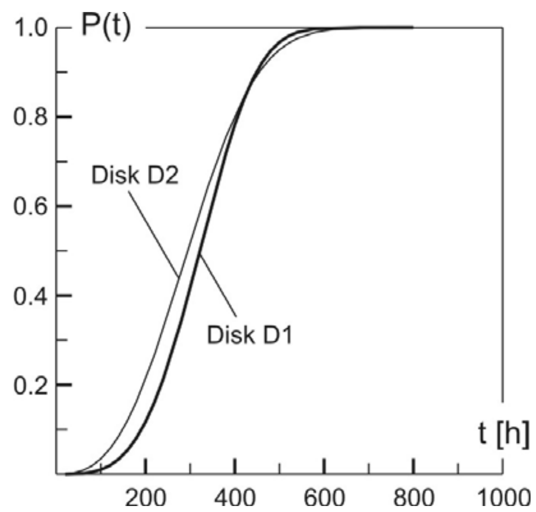

Slika 4. Verovatnoća iniciranja prsline na diskovima D1 i D2
Figure 4. Probability of crack initiation on disks D1 and D2.

Ciklične karakteristike materijala za izradu diska

Za izradu diska prvog stepena rotora kompresora niskog pritiska avionskog motora R25-300 koristi se čelik 13H11N2V2MF.

Tabela 1 sadrži ciklične karakteristike ovog čelika u termički obrađenom stanju (zagrevanje na 1000°C, kaljenje u ulju, otpuštanje na 640°C i hlađenje na vazduhu), korišćene za proračun oštećenja diska.

Cyclic properties of material for disk manufacturing

The steel 13H11N2V2MF is used for manufacturing of the first stage low pressure compressor rotor disk of R25-300 aircraft engine.

Table 1 contains cyclic properties of this steel in heat treated state (heating to 1000°C, oil quenching, tempering at 640°C and air cooling), used for damage computation of the disk.

Tabela 1. Ciklične karakteristike čelika 13H11N2V2MF u termički obrađenom stanju, /10/
Table 1. Cyclic properties of steel 13H11N2V2MF in heat treated state, /10/.

Karakteristika	Property		Vrednost	Value
Modul elastičnosti	Modulus of elasticity	E, MPa	229184,6	229184.6
Koeficijent ciklične čvrstoće	Cyclic strength coefficient	K', MPa	1140,0	1140.0
Eksponent cikličnog deformacijskog ojačavanja	Cyclic strain hardening exponent	n'	0,0579	0.0579
Koeficijent zamorne čvrstoće	Fatigue strength coefficient	σ'_f, MPa	1557,3	1557.3
Eksponent zamorne čvrstoće	Fatigue strength exponent	b	–0,0851	–0.0851
Koeficijent zamorne duktilnosti	Fatigue ductility coefficient	ε'_f	0,3175	0.3175
Eksponent zamorne duktilnosti	Fatigue ductility exponent	c	–0,7214	–0.7214

Definisanje i obrada izabranog start-stop ciklusa

U Uvodu naglašeno je da su kod diskova avionskih motora pretežno opterećenih centrifugalnim silama lopatica i sopstvenim centrifugalnim silama, značajni start-stop ciklusi motora definisani kao blokovi učestanosti obrtanja. Radi proračuna oštećenja izazvanih ovom vrstom start-stop ciklusa, za disk prvog stepena rotora kompresora niskog pritiska avionskog motora R25-300 izabran je start-stop ciklus (sl. 5) provere motora nakon ugradnje u avion, /9, 10, 12/. Taj start-stop ciklus je prikladno modifikovan i metodom rezervoara rastavljen na proste X-Y-X cikluse učestanosti obrtanja ‘n’ (sl. 6). Prosti X-Y-X ciklusi, složeni po nivou i broju pojavljivanja unutar izabranog start-stop ciklusa, navedeni su u tab. 2.

Naponsko-deformacijski odziv

Uzimajući u obzir mesto iniciranja prslina na disku prvog stepena rotora kompresora motora R25-300 bilo je dovoljno posmatrati jednu lopaticu i kritični deo pomenutog diska, ali samo postojećeg diska D2. Na početku su lopatica i kritični deo diska D2 posmatrani kao dva odvojena idealno

Defining and processing of chosen start-stop cycle

In the Introduction it has been emphasized that for aircraft engine disks, dominantly loaded by centrifugal forces of blades and own centrifugal forces, start-stop cycles defined as blocks of rotation frequency are important. For the computation of the damage produced by this kind of start-stop cycle, for the first stage low pressure compressor rotor disk of R25-300 aircraft engine, start-stop cycle (Fig. 5) of engine inspection after the assembly on aircraft, is accepted here /9, 10, 12/. This start-stop cycle is modified in a convenient way and decomposed on simple X-Y-X cycles of rotation frequency (Fig. 6). Simple X-Y-X cycles, sorted per level and number of appearing inside of selected start-stop cycle, are included in Table 2.

Stress-strain response

Taking into account the location of crack initiation on the first stage low pressure compressor rotor disk of R25-300 aircraft engine it was enough to observe one blade and disk critical part, but only of existing disk D2. At first, the blade and critical part of disk D2, were observed as two elastična tela. Primenom metode konačnih elemenata (FEM) u I-DEAS Master Series softveru, /13, 14/, određeni su naponski odzivi lopatice i kritičnog dela diska D2 za maksimalnu učestanost obrtanja $n = 186\ s^{-1}$ i dodatno za lopaticu sile koje se preko njenog korena prenose na kritični deo diska D2. Posle toga je u analizu uveden blisk D2 (disk D2 sa lopaticama) i određen je njegov osnosimetrični naponski odziv. To je pomoglo da se odredi takozvani ekvivalentni faktor koncentracije napona za tačku očekivanog iniciranja prsline na disku D2, /10/.

separate, ideal elastic bodies. Using the finite element method (FEM) in I-DEAS Master Series software, /13, 14/, stress response of blade and critical part of disk D2 are determined for maximal rotation frequency $n = 186\ s^{-1}$, and additionally for blade, the forces which through its root are transmitted onto critical part of disk D2. Hence, the blisk D2 (bladed disk D2) is involved in analysis and its axisymmetrical stress response is determined. This helped to determine the so-called equivalent stress concentration factor for point of expected crack initiation on disk D2, /10/.

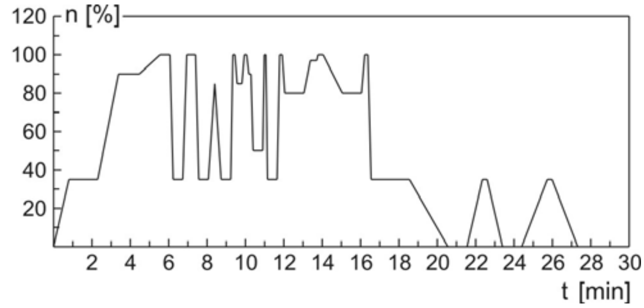

Slika 5. Izabrani start-stop ciklus
Figure 5. Chosen start-stop cycle.

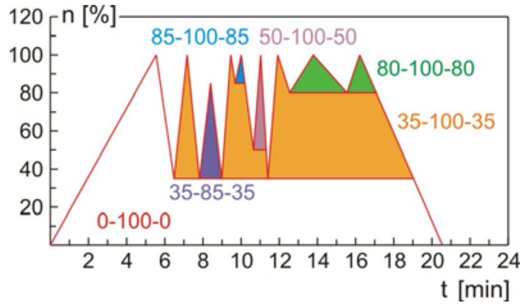

Slika 6. Modifikovan i dekomponovan start-stop ciklus
Figure 6. Modified and decomposed start-stop cycle.

Tabela 2. Prosti X-Y-X ciklusi učestanosti obrtanja unutar start-stop ciklusa
Table 2. Simple X-Y-X cycles of rotating frequencies inside of the start-stop cycle.

Nivo Level	Prosti ciklusi Simple cycles	Broj prostih ciklusa u start-stop ciklusu Number of simple cycles in a start-stop cycle
i	Xi-Yi-Xi, %	*Ni*
1	0-100-0	1
2	35-100-35	3
3	50-100-50	1
4	80-100-80	2
5	85-100-85	1
6	35-85-35	1

Naponski odziv lopatice

Model FEM za proračun naponskog odziva lopatice dat ja na sl. 7. Granične uslove čine nulta pomeranja za naznačene čvorove na kontaktnim površinama korena lopatice $u = v = w = 0$ i maksimalna učestanost obrtanja $n = 186\ s^{-1}$.

Termički obrađen čelik 13H11N2V2MF ima modul elastičnosti $E = 229184{,}6$ MPa, koeficijent Poasona $\nu = 0{,}29$ i modul klizanja $G = 88831{,}24$ MPa.

Raspodela von Mizesovih ekvivalentnih napona, za zadate granične uslove, prikazana je na sl. 8. Maksimalna vrednost ekvivalentnog napona $\sigma_{eq,\max} = 1207{,}62$ MPa vezana je za tačku očekivanog iniciranja prsline. Položaj te tačke odgovara tački realnog iniciranja prsline, /10/.

Reakcije na kontaktnim površinama korena lopatice

Podaci o reakcijama u čvorovima nultih pomeranja na kontaktnim površinama korena lopatice dobijeni su zajedno sa podacima o naponskom odzivu. Raspodela intenziteta reakcija R u tim čvorovima data je na sl. 9. Od komponenti R_{Xi} , R_{Yi} i R_{Zi} (i = 1, 2, ..., 296) formirani su posebni fajlovi, korišćeni za definisanje FEM modela za proračun naponskog odziva kritičnog dela diska D2.

Stress response of blade

FEM model for stress response computation of the blade is given in Fig. 7. Boundary conditions are zero displacements $u = v = w = 0$ for marked nodes at contact surfaces of blade root and maximal rotation frequency $n = 186\ s^{-1}$.

Heat-treated steel 13H11N2V2MF is characterised by elasticity modulus $E = 229184.6$ MPa, Poisson's coefficient $\nu = 0.29$ and shear modulus $G = 88831.24$ MPa.

Distribution of von Mises equivalent stresses for the given boundary conditions are shown in Fig. 8. Maximal value of equivalent stress $\sigma_{eq,\max} = 1207.62$ MPa is connected to the point of expected crack initiation. Position of that point corresponds to point of real crack initiation, /10/.

Reaction on contact surfaces of blade root

Data about reactions at nodes of zero displacements at contact surfaces of blade root are obtained together with data about stress response. Distribution of reactions R intensity at those nodes is given in Fig. 9. From components R_{Xi} , R_{Yi} and R_{Zi} (i = 1, 2, ..., 296) of reactions R, special files are formed used for defining of FEM model for stress response computation of the disk D2 critical part.

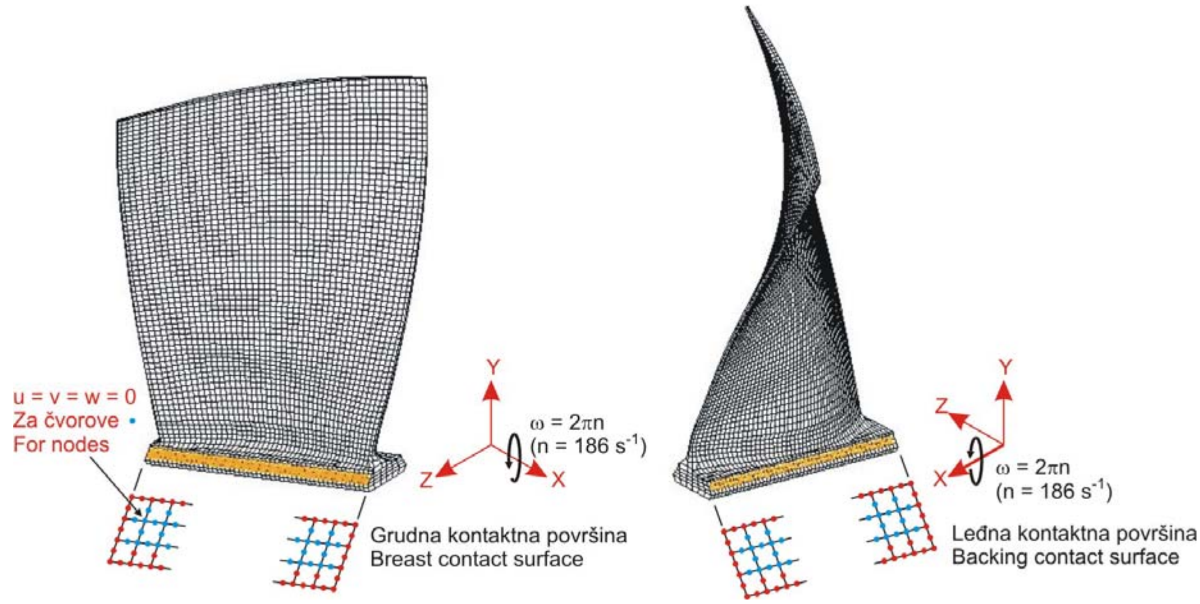

Slika 7. Model FEM za proračun naponskog odziva lopatice
Figure 7. FEM model for stress response computation of the blade.

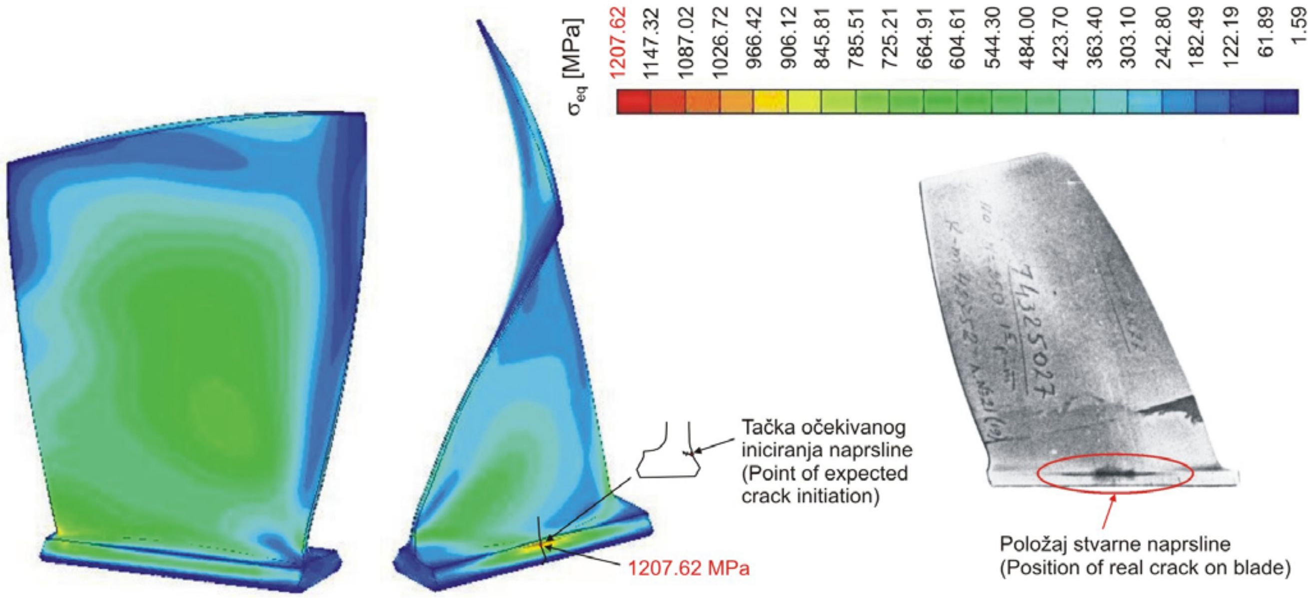

Slika 8. Raspodela von Mizesovih ekvivalentnih napona na lopatici sa primerom realne prsline
Figure 8. Distribution of von Mises equivalent stresses on blades with example of real crack.

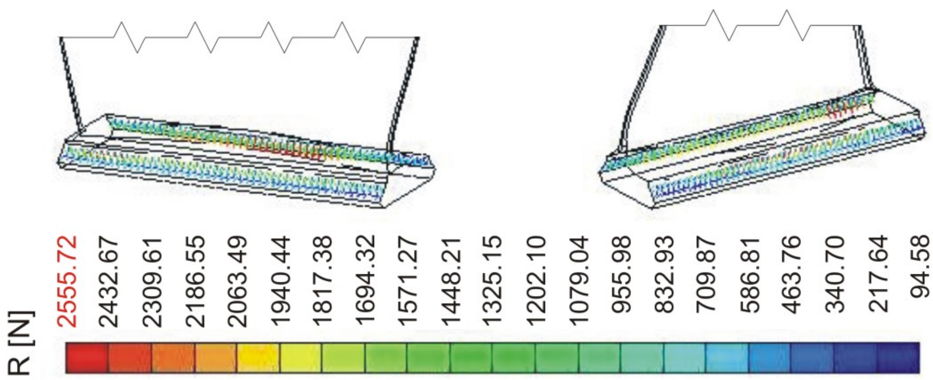

Slika 9. Raspodela intenziteta rezultanti reakcija R u čvorovima kontaktnih površina korena lopatice
Figure 9. Distribution of intensities of reactions R at nodes of contact surfaces of blade root.

Naponski odziv kritičnog dela diska D2

Model FEM za proračun naponskog odziva kritičnog dela diska D2 dat je na sl. 10. Skup graničnih uslova sadrži: nulta pomeranja čvorova na cilindričnoj površini *S* u globalnom XYZ koordinatnom sistemu, slobodna i nulta pomeranja čvorova koji pripadaju X1Y1 i X2Y2 ravnima lokalnih koordinatnih sistema X1Y1Z1 i X2Y2Z2 i koncentrisane sile F_{Xi}, F_{Yi}, F_{Zi} u označenim čvorovima kontaktnih površina elementa oboda između žljebova za vezu sa lopaticama.

Kao i kod lopatice, u svim konačnim elementima su unete karakteristike čelika 13H11N2V2MF u termički obrađenom stanju. Transformacijom reakcija R_{Xi}, R_{Yi} *i* R_{Zi} u čvorovima nultih pomeranja na kontaktnim površinama korena lopatice dobijene su koncentrisane sile F_{Xi}, F_{Yi}, F_{Zi}. Kontakt između lopatica i diska D2 je simuliran ovim silama.

Stress response of disk D2 critical part

FEM model for stress response computation of disk D2 critical part is given in Fig. 10. The set of boundary conditions contains: zero displacements of nodes on cylindrical surface S in global XYZ coordinate system, free and zero displacements of nodes on X1Y1 and X2Y2 planes of local coordinate systems X1Y1Z1 and X2Y2Z2, concentrated forces F_{Xi}, F_{Yi}, F_{Zi} in marked nodes of contact surfaces of rim elements between grooves for joint with blades.

As for blade, properties of steel 13H1N2V2MF in heat treatment state associated to all finite elements. By transformation of reactions R_{Xi}, R_{Yi} *i* R_{Zi} at nodes of zero displacements at contact surfaces of blade root, concentrated forces F_{Xi}, F_{Yi}, F_{Zi} are obtained. Contact between blades and disk D2 has been simulated by these forces.

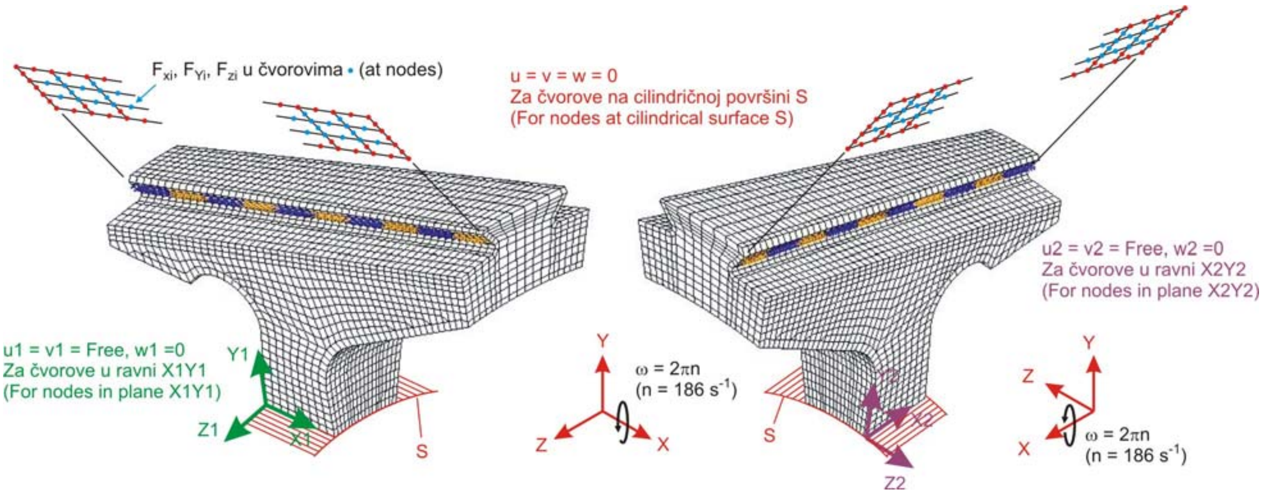

Slika 10. Model FEM za proračun naponskog odziva kritičnog dela diska D2
Figure 10. FEM model for stress response computation of disk D2 critical part.

Raspodela von Mizesovih ekvivalentnih napona prikazana je na sl. 11. Maksimalni ekvivalentni napon $\sigma_{eq,\max}$ = 1661,22 MPa je u tački očekivanog iniciranja prsline (tački P2). Položaj ove tačke odgovara tački realnog iniciranja prsline na disku D2 (sl. 2).

Distribution of von Mises equivalent stresses on critical part of disk D2 is shown in Fig. 11. Maximal equivalent stress $\sigma_{eq,\max}$ = 1661.22 MPa is at the point of the expected crack initiation (point P2). Position of this point corresponds to point of real crack initiation on disk D2 (Fig. 2).

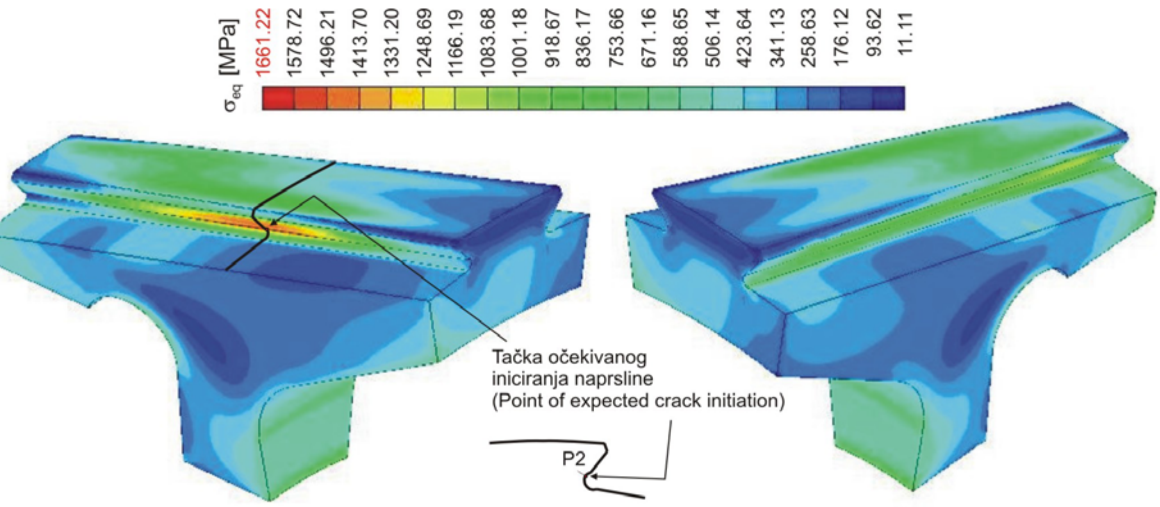

Slika 11. Raspodela von Mizesovih ekvivalentnih napona na kritičnom delu diska D2
Figure 11. Distribution of von Mises equivalent stresses on critical part of disk D2.

Osnosimetrični naponski odziv bliska D2

Model za proračun osnosimetričnog naponskog odziva bliska D2 predstavljen je na sl. 12.

Axisymmetrical stress response of blisk D2

Model for axisymmetrical stress response computation of blisk D2 is presented in Fig. 12.

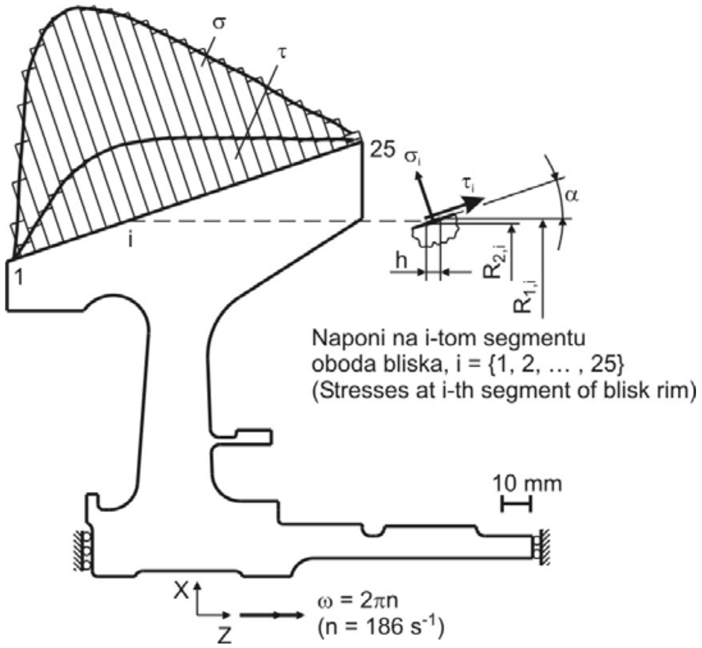

Slika 12. Model za proračun osnosimetričnog naponskog odziva bliska D2
Figure 12. Model for axisymmetrical stress response computation of blisk D2.

Granični uslovi se prema sl. 12 sastoje od napona na obodu izazvanih centrifugalnim silama integrisanih lopatica, učestanosti obrtanja $n = 186\ \mathrm{s}^{-1}$ i slobodnih pomeranja krajeva glavčine diska.

Obod bliska D2 je podeljen na 25 segmenata širine h = 5 mm. Normalni naponi σ_i i tangencijalni naponi τ_i za segment i određeni su pomoću sledećih izraza:

Boundary conditions according to Fig. 12 consist of stresses at rim produced by acting of centrifugal forces of integrated blades, rotation frequency $n = 186\ \mathrm{s}^{-1}$ and free displacement of hub disk ends.

The rim o blisk D2 is divided in 25 segments of width h = 5 mm. Normal stresses σ_i and tangential stresses τ_i for i segment are determined using the following expressions:

$$\sigma_i = \frac{z\cdot m_i\cdot R_i\left(2\pi n\right)^2}{\pi\sqrt{h^2+\left(R_{1,i}-R_{2,i}\right)^2}\left(R_{1,i}+R_{2,i}\right)}\cos\alpha\ ; \qquad \tau_i = \frac{z\cdot m_i\cdot R_i\left(2\pi n\right)^2}{\pi\sqrt{h^2+\left(R_{1,i}-R_{2,i}\right)^2}\left(R_{1,i}+R_{2,i}\right)}\sin\alpha \qquad i = 1, 2, \ldots, 25 \tag{2}$$

gde su:
z = 21 … Broj integrisanih lopatica
m_i ………Masa i-tog segmenta integrisane lopatice
R_i ………Radijus udaljenosti težišta i-tog segmenta integrisane lopatice od ose rotacije
n ....Učestanost obrtanja
α ....Ugao nagiba izvodnice koničnog oboda bliska

Imenioci razlomaka na desnim stranama izraza (2) predstavljaju površinu i-tog segmenta oboda bliska D2 jednaku površini zarubljene kupe visine h = 5 mm sa radijusom $R_{1,i}$ veće i $R_{2,i}$ manje baze. Proizvodi $[m_iR_i(2\pi n)^2]$ u datim izrazima su centrifugalne sile i-tog segmenta integrisane lopatice. Mase i položaji težišta segmenata integrisane lopatice određeni su pomoću softverskog paketa Modeler I-DEAS Master Series.

Koristeći sl. 12. i podatke o normalnim i tangencijalnim naponima na obodu bliska D2 generisan je FEM model za proračun osnosimentričnog napona. Ovaj model je sa raspodelom von Mizesovih ekvivalentnih napona dat na sl. 13.

where are:
z = 21 …..Number of integrated blades
m_i ………Mass of i-th segment of integrated blade
R_i ………Radius of gravity centre distance of integrated blade i-th segment, from rotation axis
n ……… Rotation frequency
α ……… Slope angle of generating line of conical blisk rim

Denominators of fractions on the right sides of Eqs. (2) present the surface of i-th blisk D2 rim segment, equal to surface of truncated cone h = 5 mm height with radius $R_{1,i}$ of large, and $R_{2,i}$ of small bases. Products $[m_iR_i(2\pi n)^2]$ in given expressions present centrifugal forces of i-th segment of integrated blade. Masses and positions of gravity centres of integrated blades are determined by Modeler of I-DEAS Master Series software package.

FEM model for axisymmetrical stress computation was generated using Fig. 12 and data for normal and tangential stresses at blisk D2 rim. This model with distribution of von Mises equivalent stresses is shown in Fig. 13.

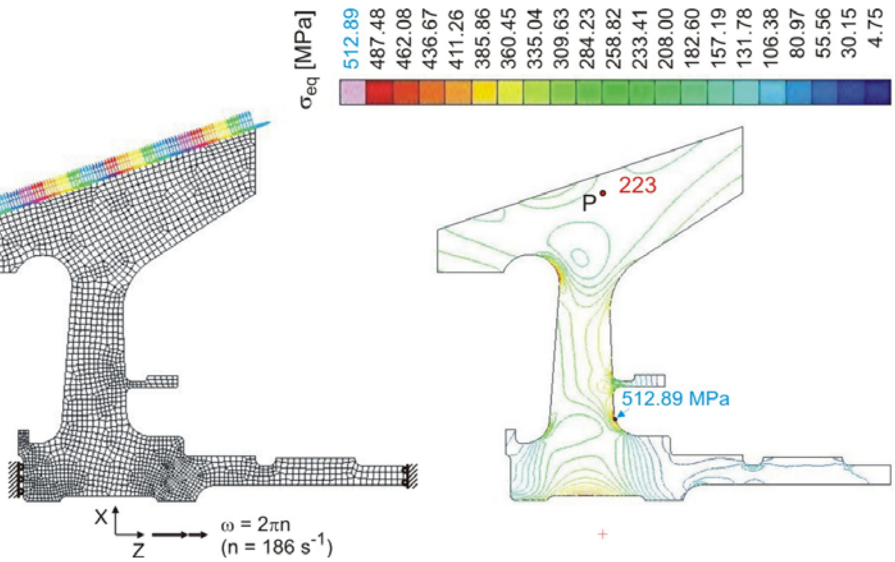

Slika 13. MKE model za proračun osnosimetričnog naponskog odziva bliska D2 sa raspodelom von Mizesovih ekvivalentnih napona
Figure 13. FEM model for axisymmetrical stress response computation of blisk D2 with distribution of von Mises equivalent stresses.

Položaj tačke P na blisku D2 odgovara položaju tačke očekivanog iniciranja prsline na disku D2. Vrednost ekvivalentnog napona u toj tački je $\sigma_{eq}(P) = 223$ MPa.

Određivanje ekvivalentnog faktora koncentracije napona

Ako se ekvivalentni napon u tački P bliska D2 (sl. 13) uzme za nominalni napon $\sigma_n = \sigma_{eq}(P) = 223$ MPa, onda se veza između tog napona i napona u tački očekivanog iniciranja prsline P2, $\sigma_{eq}(P2) = 1661{,}22$ MPa na disku D2, može uspostaviti preko ekvivalentnog faktora koncentracije napona $K_{eq} = 7{,}45$, koji predstavlja odnos $\sigma_{eq}(P2)$ i $\sigma_n = \sigma_{eq}(P)$.

Određivanje realnog naponsko-deformacijskog odziva u tački očekivanog iniciranja prsline na disku D2

Realni naponsko-deformacijski odziv u tački očekivanog iniciranja prsline na disku D2 može se opisati stabilizovanim histereznim petljama pridruženim svim i-tim X_i-Y_i-X_i ciklusima učestanosti obrtanja iz tab. 2.

Prva tačka naponsko-deformacijskog odziva koja odgovara maksimalnoj učestanosti obrtanja $n = 100\%$, određena je rešavanjem sledećeg sistema jednačina:

Position of point P on blisk D2 corresponds to position of point of expected crack initiation on disk D2. The value of equivalent stress in that point is $\sigma_{eq}(P) = 223$ MPa.

Determining of equivalent stress concentration factor

If equivalent stress at point P of blisk D2 is accepted as nominal stress $\sigma_n = \sigma_{eq}(P) = 223$ MPa, then the relation between this stress and stress in the point of expected crack initiation P2, $\sigma_{eq}(P2) = 1661.22$ MPa, on disk D2 is established by equivalent stress concentration factor $K_{eq} = 7.45$ as the ratio of $\sigma_{eq}(P2)$ and $\sigma_n = \sigma_{eq}(P)$.

Determining of real stress-strain response in the point of expected crack initiation on disk D2

Real stress-strain response in the point of expected crack initiation may be described by stabilized hysteresis loops assigned to all i-th X_i-Y_i-X_i cycles of rotation frequency from Table 2.

The first point of stress-strain response corresponding to maximal rotation frequency $n = 100\%$ is determined by solving the following system of equations:

$$\varepsilon = \frac{1}{2}\left(\frac{K_{eq}^2\sigma_{ni}^2}{\sigma E} + \frac{K_{eq}\sigma_{ni}}{E}\right); \quad \varepsilon = \frac{\sigma}{E} + \left(\frac{\sigma}{K'}\right)^{\frac{1}{n'}}; \quad i = 1 \tag{3}$$

Dimenzije ($\Delta\varepsilon\times\Delta\sigma$) stabilizovanih petlji histereza određene su rešavanjem sistema

Dimension ($\Delta\varepsilon\times\Delta\sigma$) of stabilized hysteresis loops are determined by solving the system

$$\Delta\varepsilon = \frac{1}{2}\left(\frac{K_{eq}^2\ \Delta\sigma_{ni}^2}{\Delta\sigma\ E} + \frac{K_{eq}\ \Delta\sigma_{ni}}{E}\right); \quad \Delta\varepsilon = \frac{\Delta\sigma}{E} + 2\left(\frac{\Delta\sigma}{2K'}\right)^{\frac{1}{n'}}; \quad i = 1, 2, \ldots, 6 \tag{4}$$

Prve jednačine u sistemima (3) i (4) predstavljaju dva oblika približne Sonsinoove krive, /10/, izvedene na osnovu modifikacije Nojberovog pravila, /15, 16/, (sl. 14). Druge jednačine u tim sistemima su jednačine ciklične naponsko-deformacijske krive i Masingove krive, /6, 10/.

Vrednosti za E, K' i n' u sistemima (3) i (4) su uzete iz tab. 1, a vrednosti nominalnih napona σ_{ni} i njihovi rasponi $\Delta\sigma_{ni}$ sračunati su pomoću jed. (5) i dati u tab. 3.

The first equations in the systems (3) and (4) present two forms of approximate Sonsino's curve, /10/ derived on the base of modification of Neuber's rule, /15, 16/, (Fig. 14). The second equations in those systems are equations of cyclic stress-strain curve and Masing's curve, /6, 10/.

The values for E, K' and n' in systems (3) and (4) are taken from Table 1 and the values of nominal stresses σ_{ni} and their ranges $\Delta\sigma_{ni}$ computed by Eqs, (5) are given in Table 3.

$$\sigma_{ni} = 223\left(\frac{Y_i}{100}\right)^2; \quad \sigma_{ni} = 223\left[\left(\frac{Y_i}{100}\right)^2 - \left(\frac{X_i}{100}\right)^2\right]; \quad i = 1, 2, \ldots, 6 \tag{5}$$

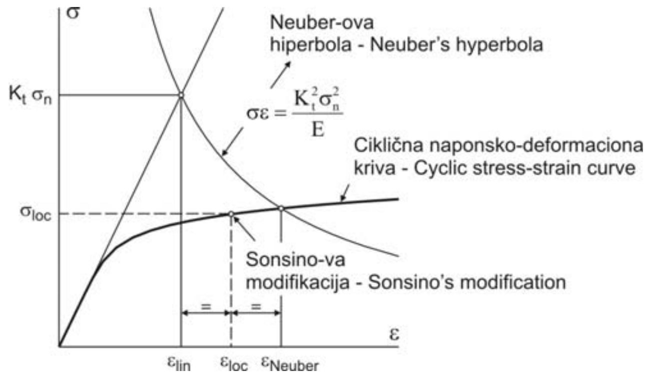

Slika 14. Sonsinoova modifikacija Nojberovog pravila
Figure 14. Sonsino's modification of Neuber's rule.

Tabela 3. Nominalni naponi σ_{ni} i njihovi rasponi $\Delta\sigma_{ni}$
Table 3. Nominal stresses σ_{ni} and their ranges $\Delta\sigma_{ni}$.

i	X_i-Y_i-X_i [%]	σ_{ni}, MPa	$\Delta\sigma_{ni}$, MPa
1	0-100-0	223.0	223.0
2	35-100-35	223.0	195.7
3	50-100-50	223.0	167.3
4	80-100-80	223.0	80.3
5	85-100-85	223.0	61.9
6	35-85-35	161.1	141.4

Sistemi jednačina (3) i (4) rešeni su grafički u Drafting modulu I-DEAS Master Series softverskog paketa. Ciklična naponsko-deformacijska kriva, Masingova kriva i približne Sonsinoove krive preslikane su u odgovarajuće B-splajn krive. Preslikavanje je izvedeno pomoću posebno napisanih fortranskih programa.

Naponsko-deformacijski odziv izazvan izabranim start-stop ciklusom, prikazan je na sl. 15, na kojoj se vide stabilizovane petlje histerezisa pridružene svim X_i-Y_i-X_i (i = 1, 2, .., 6) ciklusima učestanosti obrtanja. Masingova kriva, sem što je poslužila za određivanje dimenzija ($\Delta\varepsilon\times\Delta\sigma$) stabilizovanih petlji histereza, poslužila je i za njihovo modeliranje.

Grafički prikaz naponsko-deformacijskog odziva za ciklus 0-100-0 učestanosti obrtanja dat je na sl. 16, a numerički rezultati za taj i ostale cikluse uneti su u tab. 4.

The systems of Eqs. (3) and (4) were solved graphically in Drafting module of I-DEAS Master Series software package. Cyclic stress-strain curve, Masing's curve and approximate Sonsino's curves were copied in corresponding B-spline curves. Mapping was carried out with the help of specially written Fortran programmes.

Stress-strain response produced by chosen start-stop cycle is shown in Fig. 15, in which stabilized hysteresis loops assigned to all X_i-Y_i-X_i (i = 1, 2, ..., 6) cycles of rotation frequency can be seen. Masing's curve, except that it served for determining of dimensions ($\Delta\varepsilon\times\Delta\sigma$) of those stabilized hysteresis loops, also served for their modelling.

Graphics of stress-strain response for the cycle 0-100-0 of rotation frequency is given in Fig. 16 and numerical results for this and other cycles are given in Table 4.

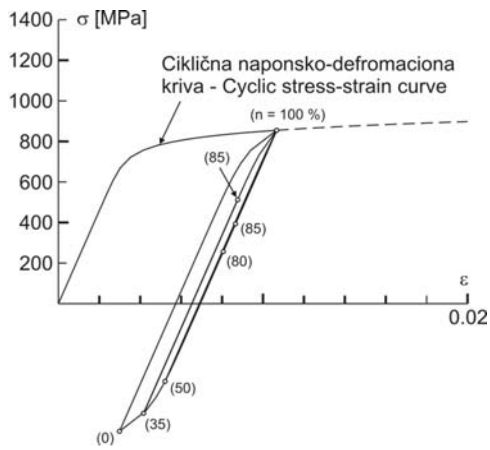

Slika 15. Naponsko-deformacijski odziv u tački očekivanog iniciranja prslina na disku D2 izazvan izabranim start-stop ciklusom
Figure 15. Stress-strain response in the point of expected crack initiation on disk D2, produced by the chosen start-stop cycle.

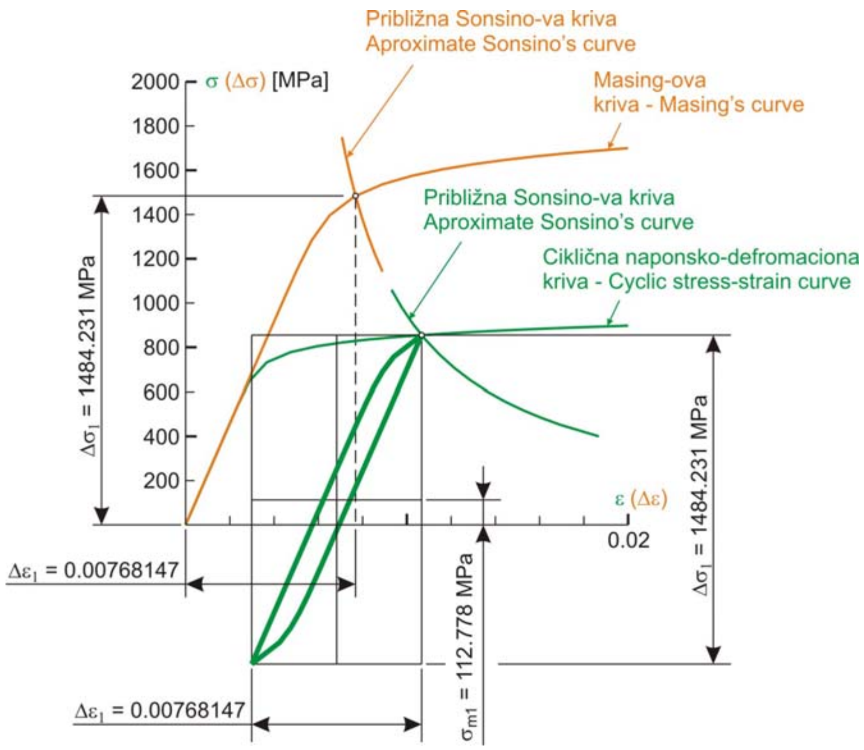

Slika 16. Naponsko-deformacijski odziv u tački očekivanog iniciranja prslina na disku D2 za 0-100-0 ciklus učestanosti obrtanja
Figure 16. Stress-strain response in the point of expected crack initiation on disk D2, produced by 0-100-0 cycle of rotation frequency.

Tabela 4. Numerički rezultati naponsko-deformacijskog odziva u tački očekivanog iniciranja prsline na disku D2
Table 4. Numerical results of stress-strain response at point of expected crack initiation on disk D2.

i	X_i-Y_i-X_i (%)	σ_{mi}	$\Delta\sigma_i$	$\Delta\varepsilon_i$	$\Delta\varepsilon_i/2$	$\sigma_{\max,i}$
1	0-100-0	112.778	1484.231	0.00768147	0.003840735	854.89
2	35-100-35	157.173	1395.440	0.00650403	0.003252015	854.89
3	50-100-50	235.722	1238.343	0.00545603	0.002728015	854.89
4	80-100-80	555.780	98.227	0.00261026	0.001305130	854.89
5	85-100-85	624.315	461.157	0.00201214	0.001006070	854.89
6	35-85-35	-14.078	1052.937	0.00459747	0.002298735	512.39

Proračun oštećenja

Oštećenje D_B izazvano blokom učestanosti obrtanja koji definiše izabran start-stop ciklus provere avionskog motora R25-300 nakon ugradnje u avion, određen je primenom Palmgren-Majnerove hipoteze o linearnoj akumulaciji oštećenja /6, 8, 10, 17-19/, matematički formulisanoj u obliku:

Damages computation

Damage D_B produced by block of rotation frequency defining chosen start-stop cycle of R25-300 aircraft engine after assembly on aircraft, was determined using Palmgreen-Miner's hypothesis of linear damage accumulation /6, 8, 10, 17-19/, mathematically formulated in the form:

$$D_B = \sum_{i=1}^{6} D_i = \sum_{i=1}^{6} \frac{N_i}{N_{fi}} \tag{6}$$

Brojevi N_i u prethodnom izrazu uzeti su iz tab. 2, dok su brojevi ciklusa do iniciranja prslina N_{fi} određeni rešavanjem sistema jednačina:

Numbers N_i in the last expression are taken from Table 2, while the numbers of cycles to crack initiation N_{fi} are determined by solving the system of equations:

$$\frac{\Delta\varepsilon}{2} = \frac{\sigma_f' - \sigma_{mi}}{E} N_f^b + \varepsilon_f' N_f^c \,; \quad \frac{\Delta\varepsilon}{2} = \frac{\Delta\varepsilon_i}{2} \,; \quad i = 1, 2, \ldots, 6 \tag{7}$$

gde prva jednačina predstavlja krive Moroua za niskociklični zamor, /6, 8, 10/.

Sistem (5) je takođe rešen grafički, korišćenjem Drafting modula I-DEAS Master Series softverskog paketa. Pomoću posebno napisanog fortranskog programa, krive Moroua su preslikane u odgovarajuće B-splajn krive. Vrednosti srednjih napona σ_{mi} i amplitude deformacija $\Delta\varepsilon_i/2$ u pomenutom sistemu, uzete su iz tab. 4.

where the first equation represents Morrow's curve for low cycle fatigue, /6, 8, 10/.

System (5) was also solved graphically using I-DEAS Master Series Software Package. With the help of a specially written Fortran programme, Morrow's curves are mapped in corresponding B-spline curves. The values of mean stresses σ_{mi} and strain amplitudes $\Delta\varepsilon_i/2$ in the mentioned system were taken from Table 4.

Primer grafičkog rešavanja sistema (5) za 0-100-0 ciklus učestanosti obrtanja, korišćenjem krive Moroua za nisko-ciklični zamor, prikazan je na sl. 17.

The example of graphical solving of system (5) for 0-100-0 cycle of rotation frequency, using Morrow's curve for low cycle fatigue, is shown in Fig. 17.

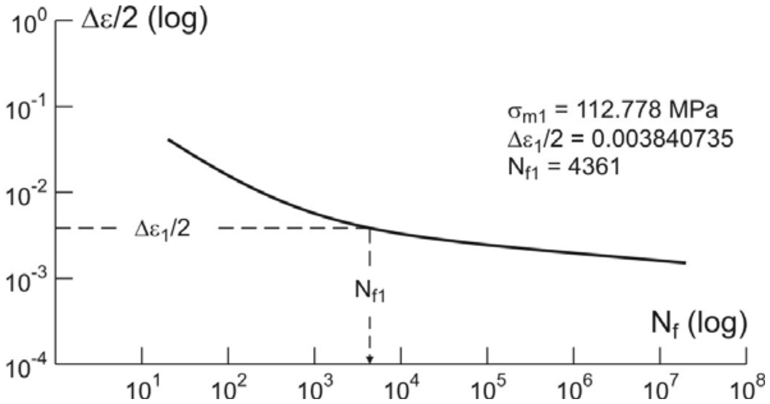

Slika 17. Primer grafičkog rešenja sistema jednačina (5) za 0-100-0 ciklus učestanosti obrtanja
Figure 17. Example of graphical solution of the system of equations (5) for 0-100-0 cycle of rotation frequency.

Tabela 5 sadrži zbirne podatke o brojevima ciklusa do iniciranja prslina N_{fi}, o oštećenjima D_i izazvanim i-tim ciklusima učestanosti obrtanja, uključujući oštećenje D_B izazvano izabranim start-stop ciklusom.

Broj ekvivalentnih 0-100-0 ciklusa učestanosti obrtanja N_B = 2,662 u razmatranom start-stop ciklusu motora dobijen je deljenjem oštećenja D_B sa oštećenjem D_1.

U slučaju ispitivanja diska D2 obrtanjem na postolju blokovima učestanosti obrtanja koji definišu ovde razmatran start-stop ciklus, iniciranje prsline bi se dogodilo nakon 1638 (= $1/D_B$) blokova ili nakon 559 časova. Važno je reći da su ovo samo procenjeni podaci.

Table 5 contains summary data about numbers of cycles to crack initiation N_{fi}, damages D_i produced by i-th cycles of rotation frequency, including damage D_B produced by chosen start-stop cycle.

Number of equivalent 0-100-0 cycles N_B = 2.662 in considered engine start-stop cycle was obtained by dividing of the damage D_B with damage D_1.

In the case of disk D2 testing by rotation in the pit, using blocks of rotation frequency which here define the considered start-stop cycle, the crack has been initiated after 1638 (= $1/D_B$) blocks or after 559 hours. It is important to say that these are only estimated data.

Tabela 5. Zbirni podaci o N_i, N_{fi}, D_i i D_B
Table 5. Summary data about N_i, N_{fi}, D_i and D_B.

i	X_i-Y_i-X_i (%)	N_i	N_{fi}	D_i
1	0-100-0	1	4361	0.00022931
2	35-100-35	3	9141	0.00032819
3	50-100-50	1	20263	0.00004935
4	80-100-80	2	1616158	0.00000124
5	85-100-85	1	139662043	0.00000007
6	35-85-35	1	434324	0.00000230
			D_B =	0.00061046

ZAKLJUČAK

Metodologija proračuna oštećenja diskova avionskih motora pretežno opterećenih centrifugalnim silama lopatica i sopstvenim centrifugalnim silama, izložena u ovom radu, može se primeniti na bilo koji start-stop ciklus definisan blokom učestanosti obrtanja. Slična metodologija može se primeniti i u slučaju kad je niskociklični zamor diskova izazvan promenljivom temperaturom.

Kompletni rezultati ovog rada mogu poslužiti za dalja istraživanja oštećenja i zamornog veka diskova avionskih motora u funkciji od geometrije i u funkciji od cikličnih karakteristika izabranog materijala. Krajnji cilj projektanata treba da je usmeren ka smanjenju mogućih oštećenja u kritičnim oblastima diskova.

CONCLUSION

Methodology of damages computation of aircraft engine disks, dominantly loaded by centrifugal forces of blades and own centrifugal forces, exposed in this paper, can be applied on whatever start-stop cycle defined by block of rotation frequency. The similar methodology can be applied in the case when the low cycle fatigue of disks is produced by variable temperature.

Complete results of this paper can serve for further investigations of damages and fatigue life of aircraft engine disks in the function of geometry and in the function of cyclic properties of selected materials. The final goal of designers should be directed to reducing of possible damages in the critical disk regions.

LITERATURA – REFERENCES

1. Mahorter, R., London, G., Fowler, S., Salvino, J., *Life Prediction Methodology for Aircraft Gas Turbine Engine Disks*, AIAA/SAE/ASME/ASEE 21st Joint Propulsion Conference, July 8-10, 1985, Monterey, California.
2. Yang, J.N., Chen, S., *An Exploratory Study of Retirement for Cause for Gas Turbine Engine Components*, Journal of Propulsion and Power 1986, Vol. 2, No.1, pp 38-49.
3. Демянушко, И.В., Темис, Ю.М., *Определение циклической долговечности при проектировании роторов авиационных ГТД*, Проблемы прочности и динамики в авиадвигателестроении, Сборник статей, Выпуск второй, Труды ЦИАМ № 996, 1982.
4. Кузменко, М., Михайлов, А., Галкин, О., *Информационные технологии проектирования на ОАО «Рыбинские Моторы»*, Ж-л Газотурбинные технологии, №2 2001 г. стр. 22-24.
5. Aircraft Accident Report – Uncontained Engine Failure Delta Air Lines Flight 1288 McDonnell Douglas MD-88, N927DA, July 6, 1996, National Transportation Safety Board, Report No. NTSB/AAR-98/01.
6. Bannantine, J.A., Comer, J., Handrock, J., Fundamentals of Material Fatigue Analysis, Prentice-Hall, Englewood Cliffs, New Jersey 1990.
7. Коллинз, Дж., Повреждение материалов в конструкциях – Анализ, Предсказание, Предотвращение, Перевод с английского, «МИР», Москва, 1984.
8. Kostaes, D., *Fatigue Behaviour and Analysis*, Talat Lecture 2401, Technische Universität München, EAA–European Aluminium Association, 1994.
9. Krčedinac, D., Dinamička izdržljivost na niskociklični zamor i procena veka rada obrtnih delova TMM, Specijalistički rad, Univerzitet u Beogradu, Mašinski fakultet, Beograd, 1993.
10. Posavljak, S., Istraživanje zamornog veka rotacionih diskova avionskih motora, Doktorska disertacija, Univerzitet u Beogradu, Mašinski fakultet, Beograd, 2008.
11. Бюллетень № 049.2.0.0221.4.АБ, Двигатель 25.
12. Radojković, R., Krčedinac, D., *Analiza i utvrđivanje prosečnog profila leta aviona u RV i PVO sa ugrađenim Motorima VIPER i MM*, Vazduhoplovni zavod „ORAO“, Sektor istraživanja i razvoja, Sarajevo 1990.
13. Lawry, M.H., I-DEAS Master Series, Mechanical CAE/CAD/CAM Software, Student Guide, Structural Dynamics Research Corporation, SDRC Part Number P-60002, 1998.
14. I-DEAS Master Series 7: Help
15. Sonsino, C.M., *Zur Bewertung des Schwingfestigkeitsverhaltens von Bauteilen mit Hilife örtlicher Beanspruchungen*, Konstruktion 45 (1993), 25-33.
16. Sonsino, C.M., Einfluss von Kaltverformungen bis 5% auf das Kurzzeitschwingfestigkeits-verhalten metallischer Werkstoffe, Dissertation, Vom Fachbereich Maschinenbau an der Technischen Hochschule Darmstadt, Darmstadt, 1982.
17. Palmgren, A., Die Lebensdauer von Kugellagern, Verfahrenstechnik, Berlin, 1924, 68, 339-341.
18. Miner, M.A., Cumulative Damage in Fatigue, Journal of Applied Mechanics, 1945, 67, A159-A164.
19. Fatemi, A., Yang, L., *Cumulative Fatigue Damage and Life Prediction Theories: A Survey of the State of the Art for Homogeneous Materials*, International Journal of Fatigue, Vol. 20, No. 1, pp. 9-34, January 1998.

INTEGRITET I VEK KONSTRUKCIJA
Zajedničko izdanje
Društva za integritet i vek konstrukcija (DIVK) i Instituta za ispitivanje materijala

STRUCTURAL INTEGRITY AND LIFE
Joint edition of the
Society for Structural Integrity and Life and the Institute for Materials Testing

http://divk.org.rs/ivk

Cenovnik oglasnog prostora u časopisu IVK za jednu godinu
(Advertising fees for one subscription year–per volume)

Kvalitet*Quality	Dimenzije*Dimensions (mm)	Cene u din.	EUR
Kolor*Colour	• obe strane*two pages 2×A4	40.000	700
	• strana*page A4/1	25.000	450
	Dostava materijala: CD (Adobe Photoshop/CorelDRAW) Print material: CD (Adobe Photoshop/CorelDRAW)		
Crno/belo*Black/White	• strana*page A4/1	12.000	250
	• ½ str A4*1/2 page A4(18×12)	8.000	150
	Dostava materijala: CD (Adobe Photoshop/Corel DRAW) Print material: CD (Adobe Photoshop/Corel DRAW)		

Pomažući članovi DIVK imaju popust od 40% navedenih cena.
(DIVK supporting members are entitled to a 40% discount on upper prices.)